 doi:10.20944/preprints201711.0082.v1

Article

Spectroscopic Evidence, Evaluation of Biological Activity and Prediction of the Safety Profile of Fatty Hydroxamic Acids Derived from Olive Oil Triacylglycerides

Monika Barbarić [1], Dražen Vikić-Topić [2], Željko Marinić [2], Danijela Bakarić [3], Marijana Zovko Končić [4], Katarina Mišković Špoljarić [5], Mirela Baus Lončar [6] and Milena Jadrijević-Mladar Takač [1,*]

[1] Department of Medicinal Chemistry, University of Zagreb, Faculty of Pharmacy and Biochemistry, A. Kovačića 1, 10000 Zagreb, Croatia ; mbarbaric@pharma.hr (M.B)
[2] NMR Centre, Ruđer Bošković Institute, Bijenička 54, 10000 Zagreb, Croatia; vikic@irb.hr (D.V.T.); zmarinic@irb.hr (Ž.M.)
[3] Division of Organic Chemistry and Biochemistry, Ruđer Bošković Institute, Bijenička 54, 10000 Zagreb, Croatia; dvojta@irb.hr (D.B.)
[4] Department of Pharmacognosy, University of Zagreb, Faculty of Pharmacy and Biochemistry, A. Kovačića 1, 10000 Zagreb, Croatia; mzovko@pharma.hr (M.Z.)
[5] Department of Medicinal Chemistry, Biochemistry and Clinical Chemistry, J. J. Strossmayer University, Faculty of Medicine, J. Huttlera 4, 31000 Osijek, Croatia; kmiskovic@mefos.hr (K. M. Š.)
[6] Division of Molecular Medicine, Ruđer Bošković Institute, Bijenička 54, 10000 Zagreb, Croatia; mbaus@irb.hr (M.B.L.)
* Correspondence: mjadrijevic@pharma.hr; Tel.: +385-1-4828-192; Fax: +385-1-6394-400

Abstract: A fatty hydroxamic acid (FHA) mixture synthesized from olive oil triacylglycerides by hydroxylaminolysis and composed predominantly of oleyl and linoleyl hydroxamic acid (OHA and LHA, respectively) was characterized by means of IR, Raman, MS and 1D and 2D ^{1}H- and ^{13}C-NMR spectroscopy. The ratio of OHA and LHA (4:1) was confirmed by MALDI TOF/TOF mass spectrometry. The radical scavenging and the Fe^{2+}-chelating activity, as well as antioxidant activity in β-carotene-linoleic acid and the Fe^{3+}-reducing power assays of the FHAs yielded positive results. The results of FHA cell toxicity on normal fibroblast (BJ) and a tumour cell line (HeLa) revealed that the normal cell line was sensitive to FHAs within the entire range of applied concentrations (5×10^{-4} mg/mL to 5×10^{-1} mg/mL), while the HeLa tumour cell line was sensitive only at the highest FHA concentration (5×10^{-1} mg/mL). *In silico* target prediction indicated cannabinoid receptors 1 and 2, the fatty-acid amide hydrolase 1 and hystone deacetylases as the most probable targets of OHA and LHA. According to ADMET predictor analysis, the safety profiles of OHA and LHA are comparable to that of SAHA (vorinostat) the histone deacetylase inhibitor in use as an antineoplastic and immunomodulating agent.

Keywords: fatty hydroxamic acids; synthesis; spectroscopy; antioxidant activity; cytotoxic activity; biological targets; ADMET; safety profile

 doi:10.20944/preprints201711.0082.v1

1. Introduction

Over the last decades there has been a rapid increase in literature dealing with the development of hydroxamic acid-based derivatives and their potential therapeutic applications as antibacterial [1-2], antifungal [3-5], antitumor [6-11], antihypertensive and antiinflammatory drugs [12]. Several hydroxamic acids (HAs) are important therapeutic agents in diverse pharmacological groups such as nonsteroidal antiinflammatory and antirheumatic drugs (*ibuproxam, oxametacib* and *bufexamac*), psychoanaleptics (*adrafinil*), antineoplastic and immunomodulating agents (*hydroxycarbamide* or *hydroxyurea, vorinostat*, *panobinostat* and *belinostat*), and iron chelating agents which are used to remove excess iron from the body in anemia and thalassemia (*deferoxamine*) [13, 14]. Recently, HAs have attracted a lot of attention as their inhibitory effect on histone deacetylases (HDACs) and the associated applicability in tumour treatment were observed [8, 10, 15-17]. Although many hydroxamic acid-based HDAC inhibitors [18] are currently in discovery and undergoing preclinical phases, the number of HDACIs that have been approved for the market still remains low.

Among the abundant available data on HAs, there is considerably less evidence about biological activity and the potential pharmacotherapeutic usefulness of monounsaturated and polyunsaturated fatty hydroxamic acids (MUFHAs and PUFHAs, respectively) that can also be of pharmaceutical and biological interest [19, 20]. FHAs can be prepared by the usual methods used to prepare HAs, *i.e.,* from fatty carboxylic acid ester or carboxylic acid chloride with either hydroxylamine or its *O*- and *N*-substituted derivatives [14, 21]. For instance, LHA was synthesized from linoleic acid (LA) *via* its reactive intermediates and hydroxylamine. The biological activity evaluation of LHA revealed that it possesses an inhibitory activity against several enzymes involved in the arachidonic acid metabolism relevant for lipid signalling in mammals, *e.g.,* various lipoxygenases and iron-containing enzymes involved in the oxygenation of polyunsaturated fatty acids (PUFAs) [22-24]. The other synthetic possibilities included convenient hydroxylaminolysis of different vegetable oils, *e.g., Jatropha Curcas* seed oil [25], canola, palm, and palm kernel oil [26--28] as well as palm olein, palm stearin, or corn oil [20]. However, owing to the diversity of fatty acids present in different vegetable oil triacylglycerides, a mixture of FHAs has been the resulting product of this type of reaction, which is difficult to separate due to the physicochemical similarities of its components. Therefore, FHAs prepared from different vegetable oils were tested as a mixture for their antimicrobial activity against *E. coli* and *S. aureus* [29-31], antifungal activity [5], and antioxidant activity [32].

The biological activity of hydroxamic acids, as well as their toxic potential is based on hydroxamic acid moiety (R-CONHOH). Metabolites such as acyl nitroso, HNO, nitric oxide, and metal complexes of the parent drug are designated as the main actors in the physiological effects [33]. The carcinogenicity and mutagenicity of HAs following toxification either *via* Lossen rearrangement to the corresponding reactive isocyanates or *via O*-sulfonation or *O*-acetylation of hydroxyl moiety to the corresponding esters of great reactivity in aqueous media have also been reported [34, 35].

Within the framework of our research on the synthesis and biological activity testing of diverse derivatives bearing the HA moiety [7, 36, 37] as well as the content determination of olive oil from autochthonous Croatian olive cultivars [38], the aim of this study was to evaluate the antioxidant and cytotoxic activity of the FHA mixture and explore the safety profile of its main components, *i.e.,* oleyl and linoleyl hydroxamic acid (OHA and LHA, respectively) *in silico.*

Preprints (www.preprints.org) | NOT PEER-REVIEWED | Posted: 14 November 2017 doi:10.20944/preprints201711.0082.v1

2. Results and Discussion

2.1. Synthesis and spectroscopic evidence

The fatty hydroxamic acid mixture (FHAs) used in this study was synthesized from olive oil triacylglycerides (TAG) by hydroxylaminolysis according to a previously published procedure (Scheme 1) [39].

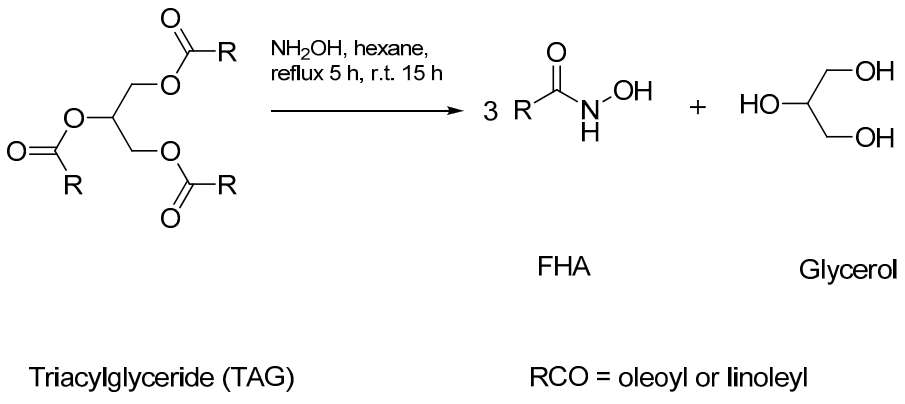

Scheme 1. The synthesis of fatty hydroxamic acids (FHAs).

The structural analysis of the obtained FHA mixture was carried out by FTIR, Raman, one- and two-dimensional, homo- and hetero-nuclear ^{1}H- and ^{13}C-NMR spectroscopy, and by MALDI-TOF-TOF mass spectrometry. Here we report the main findings.

Since oleic acid (OA, 18:1n-9) is the most abundant monounsaturated fatty acid (MUFA) and linoleic acid (LA,18:2n-6) the most abundant polyunsaturated fatty acid (PUFA) in olive oil triacylglycerides (TAG), where their concentrations in the total content of fatty acids (FAs) range from 55% to 83% for OA and from 3.5% to 21.0% for LA [40], their corresponding hydroxamic acids were expected to be present in the reaction product, *i.e.*, FHAs. And the question that has arisen is whether there are certain discernible amounts of LHA and/or other PUFHAs in addition to OHA in the synthesized FHAs mixture that may be of relevance for biological effects because small amounts of other PUFAs may also be present in olive oil TAGs, *e.g.*, linolenic acid (LNA, 18.3n-6) in 0.4% to 1.9%, while eicosanoic acids are present in trace amounts. As it is the case with the separation of MUFAa and PUFAs due to similarities in their physicochemical properties [41], we encountered such difficulty with our FHA mixture and therefore continued to study FHAs with different spectroscopic methods in order to elucidate its main components.

2.1.1. FTIR and Raman spectroscopy

The FTIR spectra of precursor olive oil and FHAs are presented in Figure S1 and the most significant bands of FHAs in Table S1 in the supplementary material. The FTIR results provided clear and convincing evidence regarding the chemical structure of FHAs, mainly from amide type carbonyl and OH/NH stretching bands. The broad band from ν 3650 cm^{-1} to 2500 cm^{-1} corresponds

Preprints (www.preprints.org) | NOT PEER-REVIEWED | Posted: 14 November 2017 doi:10.20944/preprints201711.0082.v1

to –CONHOH moiety, and the peak at ν 3285 cm^{-1} was assigned to N-H stretching vibrations. The O-H moiety in -CONHOH group was most likely associated *via* inter- and/or intra-molecular hydrogen bonds and due to that produced a very broad vibration that overlapped with the stretching of the methyl and methylene groups. In addition to these findings, in the FTIR spectrum of the FHAs there were two stretching vibrations for the C=O group at ν 1664 cm^{-1} and 1624 cm^{-1} that belonged to amide I and amide II vibrations, respectively. The weak band at ν 3001 cm^{-1} originated from =C-H stretching, thus indicating the presence of one or more unsaturated moieties in the alkyl chain. Vibration bands of the methyl group appeared at 2952 cm^{-1} and 2872 cm^{-1}, while stretching bands of methylene groups appeared at 2918 cm^{-1} and 2849 cm^{-1}. Strong and medium bands at 1464 cm^{-1} and 1441 cm^{-1}, respectively, were attributed to the deformation of C-H groups, while the medium strong band at 1096 cm^{-1}, may have been due to skeletal vibrations, *e.g.*, the stretching of –C-C- bonds.

The most intense bands in the Raman spectrum of the FHAs (Table S1 in supplementary material) have to do with the stretching of the CH_2 groups, ν_{as} 2932 cm^{-1} and ν_{sym} 2847 cm^{-1}. The C=O stretching produced two bands that arose due to the stretching of the C=O group of amide moiety in the Raman spectrum of the FHAs, the medium one at 1659 cm^{-1} and one very weak band at 1622 cm^{-1}. The bending of the C-H bond in the methylene group appeared at 1441 cm^{-1} as a very strong and broad band. The strong band at 1295 cm^{-1} most likely arose due to C-N stretching. The stretching of the -C-C- group of medium intensity appeared at 1095 cm^{-1} and 1062 cm^{-1}. Bands at lower wavenumbers were either weak or very weak. FTIR and Raman spectra of the FHAs may be useful for the assessment of unsaturated moieties from which the FHAs mixture was composed. Band positions and/or band shapes attributed to the stretching and/or bending modes that include an H-atom imply the presence of hydrogen bonds.

2.1.2. NMR spectroscopy

The ^{1}H-NMR spectrum of the FHA mixture (in $CDCl_3$) and chemical structures of its main components, *i.e.,* OHA and LHA, with labelled proton atoms are displayed in Figure S2 and Table S2 in the supplementary material. Analogous protons in LHA are labelled with an asterisk (*) (Figure S2, Table S2). The proton assignments were made on the basis of observed chemical shifts (δ ppm) in the 1D ^{1}H-NMR spectrum and 2D HMQC (Heteronuclear Multiple Quantum Coherence), 2D HMBC (Heteronuclear Multiple Bond Coherence) and ^{1}H-^{1}H COSY (Correlated spectroscopy) experiments (Figure S2, Figure S4, Figure S5 and Figure S6, respectively), as well. The observed chemical shifts were in good agreement with the available literature data [42, 25]. The ^{1}H-NMR spectrum of the FHAs was characterized by eight signals that belong to eight chemically and magnetically nonequivalent protons. Protons of the –CO-NHOH group were observed as a broad and very week signal at δ 8.674 ppm, while the multiplet signal at δ 5.339 ppm was assigned to olefinic protons (-HC=CH-) in OHA (H9, H10) and LHA (H9*, H10*, H12* and H13*). The signal at δ 0.880 ppm (t) was assigned to protons in the methyl groups, *i.e.,* H-18 and H-18*. Methylene protons (-CH_2-) in the OHA (H2, H3, H4 to H7, H8, H11, H12 to H17) and in LHA (H2*, H3*, H4* to H7*, H8*, H11*, H15* to H17) were observed from δ 1.254 to 2.777 ppm depending on the position of each methylene group in the alkyl chains of the FHAs. Thus methylene protons H4 to H7, H12 to H17, H4* to H7*, H15* to H17* were observed at δ 1.250 to 1.290 ppm (m) while methylene protons

Preprints (www.preprints.org) | NOT PEER-REVIEWED | Posted: 14 November 2017 doi:10.20944/preprints201711.0082.v1

H8, H11, H8* and H14*, adjacent to the olefinic bond, *i.e.,* -C$\underline{H_2}$-CH=CH- were observed as multiplet (m) at δ 1.988 to 2.040 ppm. Methylene protons H2 and H2*, in the immediate vicinity to the -CO-NHOH group were observed downfield as a triplet (t) at δ 2.135 ppm and methylene protons H3 and H3* at 1.621 ppm (m). However, a triplet (t) signal of very low intensity at δ 2.766 ppm indicated the presence of LHA and this signal corresponds to methylene protons H11*. Although this signal may come from LHA (-CH=CH-C$\underline{\mathbf{H_2}}$-CH=CH-) and/or LNHA (–CH=CH-**C**$\underline{\mathbf{H_2}}$-CH=CH-**C**$\underline{\mathbf{H_2}}$-CH=CH-) and these signals may be overlap to some extent, the assignation was made in favour of LHA methylene protons H11* because of the lack of an additional characteristic signal of methyl protons (–C$\underline{H_3}$) of LNA (n-3) which is usually separated from –C$\underline{H_3}$ of n-9 and n-6 FAs and was found to be at δ 0.970 ppm compared to oleoyl and linoleyl methyl protons observed at δ 0.880 ppm [43, 44].

On the basis of these findings, it was concluded that the obtained FHAs mixture was either free of LNHA or its minor presence was below the discernible amount relevant to the ^{1}HNMR spectroscopy.

The experimental ^{13}C-NMR data of FHAs recorded in deuterated chloroform ($CDCl_3$) (Figure S3 in supplementary material) and theoretical data computed for OHA and LHA using nmrshiftdb (http://nmrshiftdb.nmr.uni-koeln.de) and ChemDraw Ultra v. 11.0 ^{13}C NMR software packages, together with available literature data for ^{13}C-NMR of LHA are presented in Table S2 in the supplementary material. Analysis of the ^{13}C-NMR spectrum of FHAs confirmed the presence of signals characteristic for 18:1 and 18:2 FHAs (Figure 1). The distinction and assignments of carbon atoms that belong to OHA from those of LHA were made on the basis of characteristic chemical shifts (δ ppm), signal intensities, and by comparing experimental data with the computed theoretical spectra of OHA and LHA, as well as with the available literature data for ^{13}C-NMR of LHA [24]. The carbon atoms involved in the carbonyl (C=O) and methyl (– CH_3) groups were observed as singlets at δ 171.73 and 13.99 ppm, respectively, for both, OHA and LHA, while all other carbon atoms were separated with intensities that were in favour of the OHA as a predominant component in the FHA mixture. The observed six signals of olefinic carbon atoms in the region of δ 127.78 to 130.14 ppm (Table S2, Figure 1) in the ^{13}C-NMR spectrum of FHAs indicated the presence of six nonequivalent carbon atoms involved in the C=C bonds. Although ^{13}C-NMR cannot be considered a quantitative technique compared to ^{1}H-NMR, the observed signals at distinct chemical shifts with obviously different signal intensities were assigned so that the OHA (C9, δ 129.56 ppm and C10, 129.94 ppm) was determined as the prevailing component of FHAs with lower proportions of LHA (C9*, C10*, C12* and C13*, δ 129.86, 127.78, 130.14 and 127.99, respectively). No signs of inadvertent *Z*→*E* isomerization of OHA and LHA during the synthesis were observed.

Preprints (www.preprints.org) | NOT PEER-REVIEWED | Posted: 14 November 2017 doi:10.20944/preprints201711.0082.v1

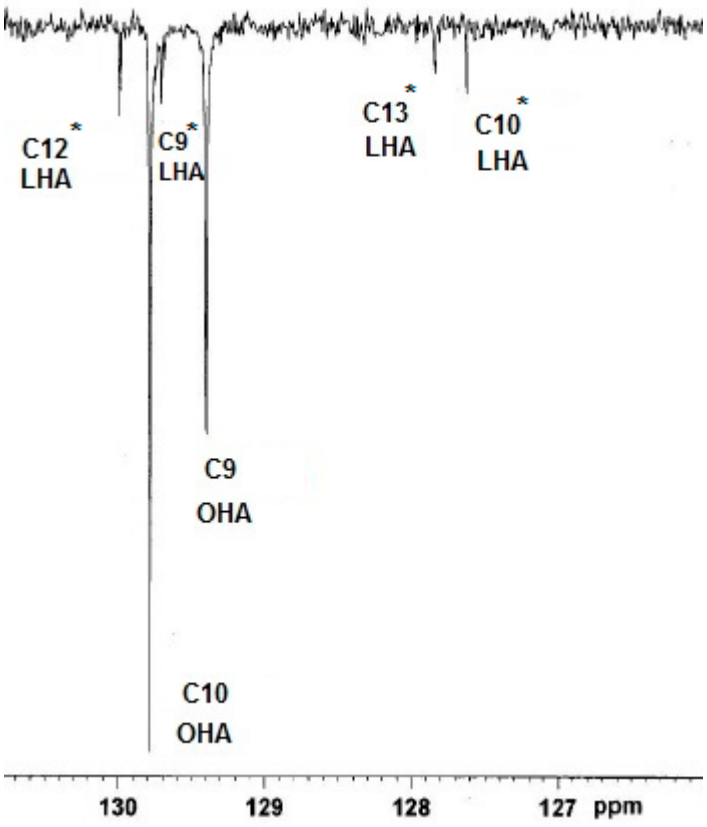

Figure 1. A part of ^{13}C APT (Attached-Proton-Test) spectrum of FHAs mixture recorded in $CDCl_3$, displaying olefinic carbons of OHA (a pair of larger signals, *i.e.*, C9 129.56 ppm and C10 129.94 ppm) and LHA (two pairs of smaller signals, *i.e.*, C9* 129.86, C10* 127.78, C12* 13014 and C13* 127.99 ppm).

Obviously, NMR techniques alone were not able to provide detailed information about the molar proportion of different fatty hydroxamic acids in the FHA mixture which was also due to the fact that NMR is a less sensitive technique compared to traditional chromatographic methods and mass spectrometry. Therefore, we continued to study the FHA mixture by matrix-assisted laser desorption/ionization (MALDI) time-of-flight/time-of-flight (TOF-TOF) high resolution tandem mass spectrometry (MS).

2.1.3. MALDI-TOF/TOF MS spectrometry

In order to obtain a more precise ratio of components in the FHA mixture, MALDI-TOF-TOF MS was applied. A part of the MALDI-TOF/TOF tandem mass spectrum of synthesized FHAs in the region of mono- and polyunsaturated FHAs, *i.e.*, m/z 310 – 325, is presented in Figure 2. A broader MS spectrum is presented in Figure S7 in the supplementary material, as well. Components of the FHA mixture, *i.e.*, OHA and LHA were observed as singly charged sodium alkali adducts, therefore their molecular ions were shifted by the mass of sodium, *i.e.*, 22.99. Thus the molecular ions of the predominantly present OHA were observed as their sodium adducts $[M + Na]^+$ at m/z 320.25 and $[M + Na + H]^+$ at m/z 321.25 while molecular ions of LHA, *i.e.*, $[LHA + Na]^+$ at 318.24 and $[LHA + Na + H]^+$ at 319.24. The ratio of the two main m/z intensities, *i.e.*, $I_{m/z\ [OHA + Na]+}$ / $I_{m/z\ [LHA + Na]+}$ was found to be 4:1. On the basis of the results of the MALDI TOF/TOF MS analysis it was

Preprints (www.preprints.org) | NOT PEER-REVIEWED | Posted: 14 November 2017 doi:10.20944/preprints201711.0082.v1

concluded that the amount of LHA in the FHA mixture was 20% and of OHA 80%. The signal at m/z 322.25 was attributed to the $[OHA + Na + 2H]^+$ however, the possible presence of saturated stearic hydroxamic acid (SHA) due to its presence in olive oil TAG (0.5% to 5.0%) cannot be completely excluded through this finding since its molecular ion sodium adduct m/z $[SHA + Na]^+$ has the same m/z as $[OHA + Na + 2H]^+$.

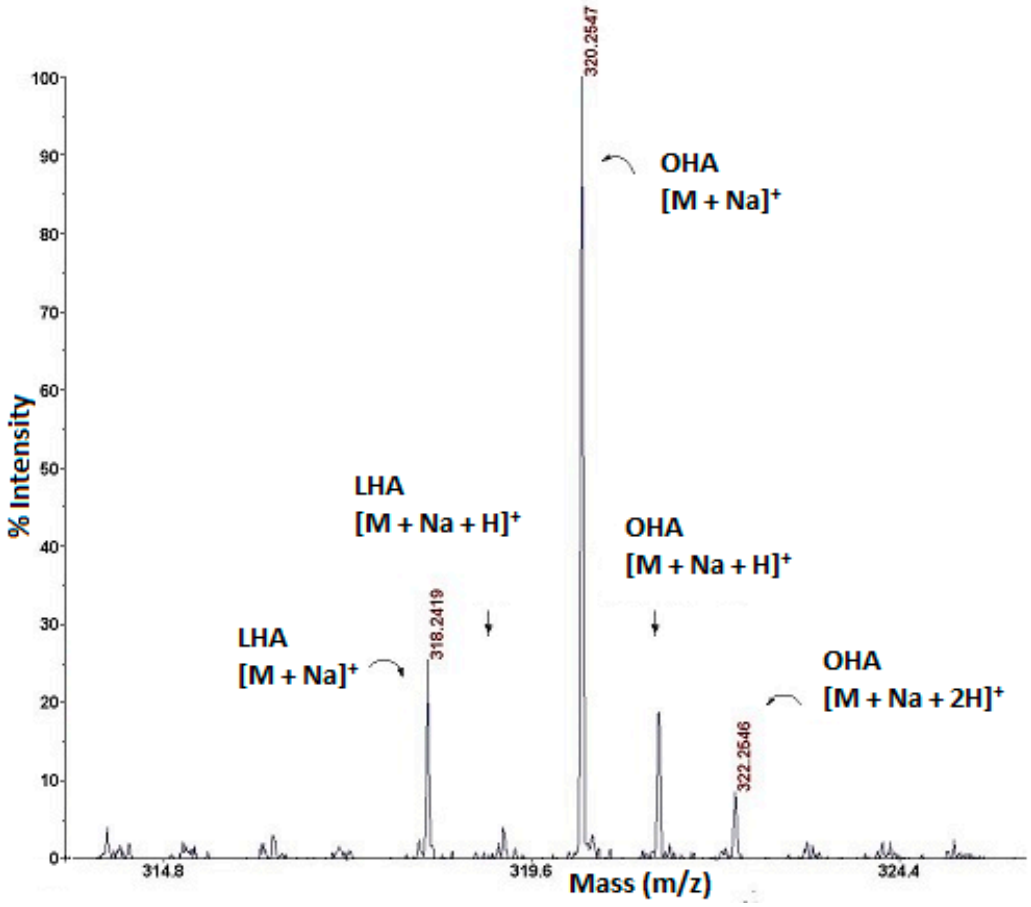

Figure 2. A part of the MALDI-TOF/TOF tandem mass spectrum of the FHA mixture in the region of m/z 314.0 – 325.0 with molecular ions of OHA and LHA represented as their sodium alkali adducts $[M + Na]^+$, $[M + Na + H]^+$ and $[M + Na + 2H]^+$.

2.2. Biological evaluation in vitro

So far, FHA products prepared from different plant oils have been evaluated for their biological activity mostly without specifying the exact composition of the mixture, and so have asserted that the fatty hydroxamic acid (FHA) from the seed oil of *Cyperus esculentus* showed antioxidant activity tested by DPPH radical scavenging assay as the concentration reduced below 0.05 mg/mL while the antioxidant capacity reduced once the concentration became higher and FHA tended toward being a pro-oxidant. *C. esculentus* has been also presented as a potential source of feed stock for the synthesis of a relatively cheap and non-toxic FHA [32]. Here we report the antioxidant and cytotoxic activity of a FHA mixture obtained from olive oil triacylgycerides with its main components OHA and LHA (80 : 20, ww).

 doi:10.20944/preprints201711.0082.v1

248
249 *2.2.1. Antioxidant activity*
250
251 Four different methods for the assessment of FHA antioxidant activity were used in this study:
252 radical scavenging activity (RSA), chelating activity of Fe^{2+} ions (ChA), antioxidant activity in
253 β-carotene bleaching assay (AOA), and the reducing power assay (RP).
254 The capability of FHAs to scavenge free radicals was assessed in reaction with the relatively
255 stable 1,1-diphenyl-2-picrylhydrazyl (DPPH) free radical. FHAs demonstrated notable antiradical
256 activity, albeit lower than butylated hydroxyanisol (BHA), a widely used food antioxidant. The
257 obtained result for FHAs, RSA EC_{50} = 235.66 ± 54.01 μg/mL, corresponds to the concentration that
258 scavenges 50% of the DPPH free radicals present in the solution (Table 1).
259 The chelation of metal ions (ChA) such as copper and especially iron ions by certain
260 compounds decreases their pro-oxidant activity [45]. This aspect of antioxidant activity is
261 particularly important because in the Fenton reaction hydroxyl radical production is directly
262 related to the concentration of the iron ion or other transition ions [46]. The results are expressed as
263 ChA EC_{50}, the concentration that chelates 50% of the Fe^{2+} ions present in the solution. In this study
264 the chelating activity of FHAs was compared with two chelating standards,
265 ethylenediaminetetraacetic acid (EDTA) and quercetin (Qn) (Table 1). FHAs showed lower activity
266 (ChA EC_{50} = 1226.53 ± 58.33 μg/mL) than the strong ion chelator, EDTA (ChA EC_{50} = 12.64 ± 2.81
267 μg/mL). However, the FHA mixture was as active as Qn (EC_{50} = 1177.96 ± 175.73 μg/mL), a natural
268 ion chelator, present in many types of fruits and vegetables.
269 Antioxidant activity in β-carotene linoleic acid assay is frequently employed as a test for
270 measuring total antioxidant activity (AOA) of plant extracts by the oxidation of the aqueous
271 emulsion of β-carotene and linoleic acid [47, 48]. This assay measures the capacity of antioxidants to
272 inhibit the formation of conjugated diene hydroperoxide arising from linoleic acid oxidation. Thus,
273 the assay gives insight into the inhibitory effect of substances on lipid peroxidation [49].
274 Antioxidant activity is expressed as percentage (%) of inhibition relative to the control and AOA
275 EC_{50} (μg/mL) is defined as the concentration of an antioxidant required to inhibit the 50%
276 degradation of beta-carotene relative to the control under the given experimental conditions. The
277 FHA concentration (AOA EC_{50} = 55.71 ± 1.29 μg/mL) (Table 1) showed that the FHAs were able to
278 significantly reduce the rate of degradation of β-carotene in comparison with water as control.
279 However, FHAs activity is comparable but somewhat lower than the activity of BHA (AOA EC_{50} =
280 45.61 ± 0.11 μg/mL) (Figure 3, Table 1).

Preprints (www.preprints.org) | NOT PEER-REVIEWED | Posted: 14 November 2017 doi:10.20944/preprints201711.0082.v1

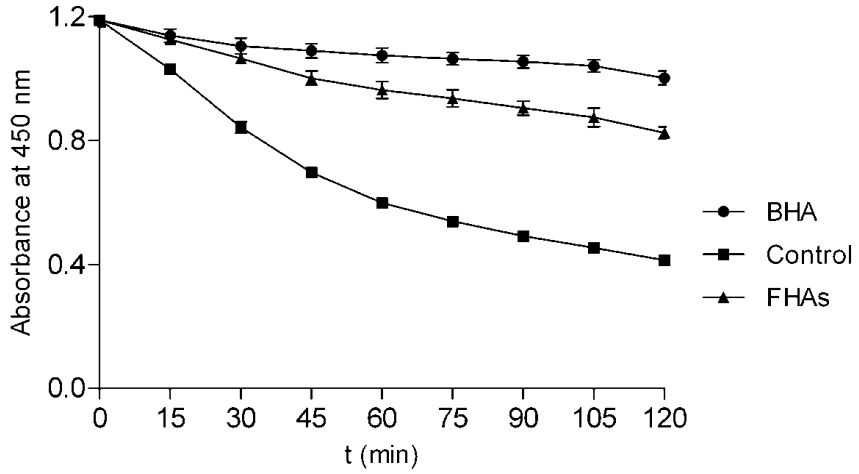

Figure 3. Inhibition of β-carotene-linoleic acid emulsion bleaching by the FHAs and BHA. Values are presented as mean ± SD (n = 3).

Literature reports suggest that the antioxidant activity of some antioxidants and plant extracts is associated with their reducing power (RP $EC_{0.5}$) which terminates free radical chain reactions [50]. The reducing power of the investigated FHAs mixture increased linearly with the concentration (Figure 4). Coefficients of determination (r^2) for ascorbic acid (Asc) and FHAs were 0.9807 and 0.9166, respectively. In this assay, ascorbic acid demonstrated significantly better reducing power (RP $EC_{0.5}$ = 97.028 ±10.87 µg/mL) than FHAs (RP $EC_{0.5}$ = 395.71 ± 47.37 µg/mL) (Table 1). The RP $EC_{0.5}$ as a sample concentration providing 0.5 of absorbance (EC_{50}) was calculated by plotting absorbance at 700 nm against the corresponding sample concentration.

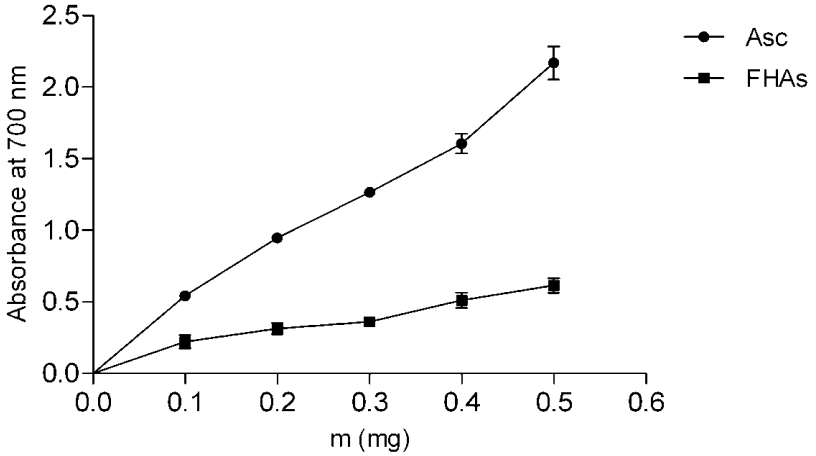

Figure 4. Reducing power activities of FHAs and ascorbic acid (Asc). Values are presented as mean ± SD (n = 3).

Preprints (www.preprints.org) | NOT PEER-REVIEWED | Posted: 14 November 2017 doi:10.20944/preprints201711.0082.v1

Table 1. The results of DPPH radical scavenging activity (RSA EC_{50}), Fe^{2+} chelating activity (Ch EC_{50}), antioxidant activity in β-carotene-linoleic acid assay (AOA EC_{50}) and Fe^{3+}reducing power (RP $EC_{0.5}$) of FHAs composed of OHA and LHA (4 : 1). Values (μg/ml) are presented as means ± SD (n = 3).

Sample	RSA EC_{50} (μg/mL)	ChA EC_{50} (μg/mL)	AOA EC_{50} (μg/mL)	RP $EC_{0.5}$ (μg/mL)
FHAs	235.66 ± 54.01 [1*]	1226.53 ± 58.33 [2*]	55.71 ± 1.29 [1*]	395.71 ± 47.37 [3*]
Standard	24.46 ± 2.54 [1]	12.64 ± 2.81 [2] 1177.96 ± 175.73 [4]	45.61 ± 0.11 [1]	97.028 ±10.87 [3]

[1] Butylated hydroxyanisol

[2] EDTA

[3] Ascorbic acid

[4] Quercetin

[*] Statistical differences with the corresponding standards ($P < 0.05$) within the column.

The results of these studies demonstrated that the FHA mixture possessed moderate antioxidant activity.

2.2.2. Cytotoxic activity

The results of the MTT colorimetric assay revealed that the addition of the FHAs to normal (BJ) and tumour (HeLa) cell lines at a final concentration of 0.5 mg/mL suppressed the cell growth of both of the tested lines by more than 90% (Figure 5). The antiproliferative effect on the normal cell line at 0.05 mg/mL was strong (92% of cell died), while moderate growth suppression (8% of dead cells) was observed in the tumour cell line. The BJ and Hela cell line have different modes of biological response to the FHAs applied at the tested concentration, *i.e.*, the growth of normal cells was strongly suppressed while the tested tumour cell line was not as sensitive. The established IC_{50} value for HeLa (80.5 μg/mL) and BJ (7.92 μg/mL) confirmed a ten times higher FHA cytotoxicity for normal cells compared with malignant HeLa cells.

Preprints (www.preprints.org) | NOT PEER-REVIEWED | Posted: 14 November 2017 doi:10.20944/preprints201711.0082.v1

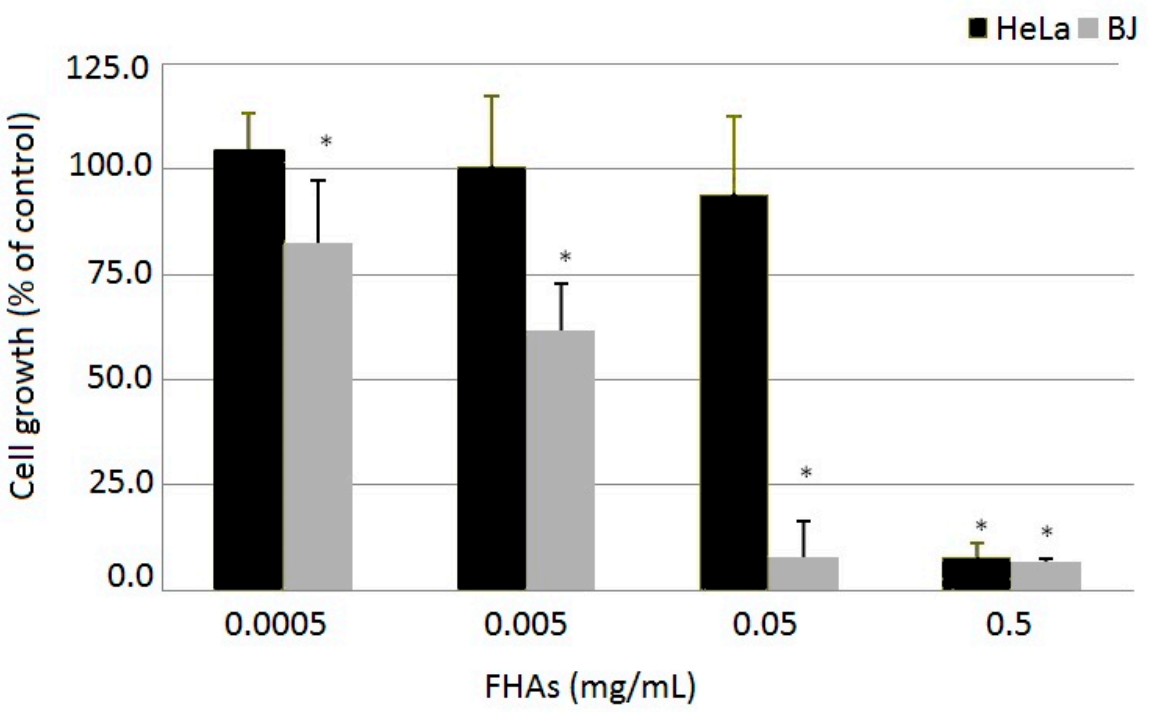

Figure 5. The cytotoxic effects of the FHAs. Cell line growth is displayed as percentage (%) after 72 h of incubation at the final concentration range (0.0005 - 0.5 mg/mL) evaluated by MTT colorimetric technique. Data represent the mean value of three independent experiments done in triplicate. Statistically significant change ($p < 0.05$) is presented by an asterisk (*).

2.3. *In silico* prediction of biological targets and safety profile

2.3.1. *Target prediction*

Potential biological on- and off-targets of OHA and LHA molecules were evaluated by the SwissTargetPrediction web server that provides a prediction for small molecules using a combination of 2D and 3D similarity measures (http://www.swisstargetprediction.ch). It compares the query molecule against a library of 280000 compounds active on more than 2000 targets of 5 different organisms [51, 52]. The outcome of this analysis yielded fifteen of the most probable targets in *Homo sapiens* for each query molecule. Three main target classes were revealed: the 'enzyme other' with an overall frequency of 80% for OHA and 87% for LHA, the 'membrane receptor' class with a frequency of 13% for both OHA and LHA, and the 'ion channel' class with a 7% frequency for OHA. The revealed specific targets and their probabilities are displayed in Table 2.

In addition to histone deacetylases 1 to 9 (HDAC1 – HDAC9) with probabilities (P) from 0.4 to 0.5 for both OHA and LHA, the most probable targets that include cannabinoid receptor 1 (CB1) (P = 0.6 for OHA and 0.8 for LHA) and cannabinoid receptor 2 (CB2) (P = 0.4 for OHA and 0.3 for LHA) as well as fatty-acid amide hydrolase 1 (FAAH) (P = 0.6 for OHA and 0.5 for LHA) were also predicted (Table 2). The prediction for SAHA (suberoylanilide hydroxamic acid, vorinostat) the first

Preprints (www.preprints.org) | NOT PEER-REVIEWED | Posted: 14 November 2017 doi:10.20944/preprints201711.0082.v1

HDAC inhibitor registered by the FDA, revealed that histone decetylases 1 to 11 (HDAC1 - HDAC11) are the main targets of this molecule with the highest probability (P = 1.0). Although not as high, the probabilities of interactions of OHA and FHA with histone deacetylases could be a good starting point for further research regarding the development of more prominent HDAC inhibitor properties for tumour treatment. Chemical structures of oleoyl hydroxamic acid (OHA), linoleyl hydroxamic acid (LHA) and suberoylailide hydroxamic acid (SAHA) are displayed in Figure 6.

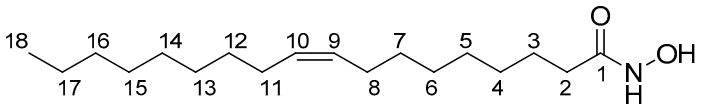

Oleoyl hydroxamic acid (OHA)

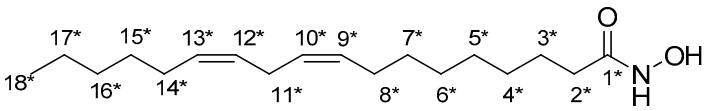

Linoleyl hydroxamic acid (LHA)

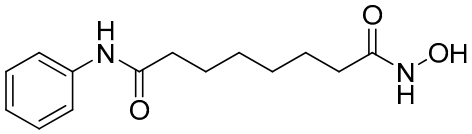

Vorinostat (Suberoylanilide hydroxamic acid, SAHA)

Figure 6. Chemical structures of oleoyl hydroxamic acid (OHA), linoleyl hydroxamic acid (LHA) and suberoylailide hydroxamic acid (SAHA)

The probability of interactions with FAAH in humans assumes the inhibition of this enzyme, which is involved in hydrolytic degradation of endogenous fatty acid amides (FAAs) and among them the signalling endocannabinoid molecule anandamide (*N*-arachidonoylethanolamine, AEA) to arachidonic acid and ethanolamine [53, 54], as well as oleamide (*cis*-9,10-octadecanoamide, ODA), the primary amide of oleic acid which is an endogenous sleep-inducing substance, to oleic acid and ammonia [55].

Anandamide was also found in chocolate together with two substances that might mimic the effects of anandamide, *N*-oleoylethanolamide (OEA) and *N*-linoleoylethanolamide (LEA) [56]. More recently, many new molecules have been investigated as possible FAAH inhibitors [57]. From the predicted interactions of OHA and LHA with CB1 and CB2, as well as with FAAH, it could be assumed that these molecules may also mimic the effects of *N*-oleoylethanolamide and *N*-linoleoylethanolamide on anandamide, as well as oleamide in the body based on their similarities with these endogenous messengers.

By increasing the anandamide level, its physiological effects either in the central or peripheral nervous system, *via* cannabinoid receptors CB1 or CB2, respectively, will consequently be increased

Preprints (www.preprints.org) | NOT PEER-REVIEWED | Posted: 14 November 2017 doi:10.20944/preprints201711.0082.v1

as will the influence on its many physiological functions to *e.g.*, eating, sleep patterns or pain *via* CB1 as well as immunity, mainly via CB2 receptors. The potential metabolic pathways of FAAs normally present in the body (**1** – OEA, **2** – LEA, **3** – OA and **4** – LA) as well as xenobiotic OHA (**5**) and LHA (**6**) are displayed in Scheme 2.

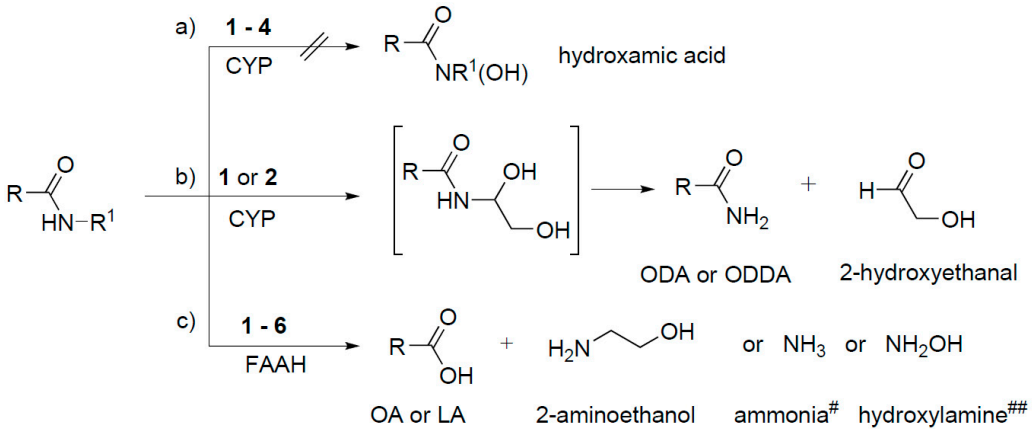

1 RCO = oleoyl, R^1 = CH_2CH_2OH, *N*-oleoylethanolamide (OEA)
2 RCO = linoleyl, R^1 = CH_2CH_2OH, *N*-linoleoylethanolamide (LEA)
3 RCO = oleoyl, R^1 = H, oleamide (9-octadecadienamide, ODA)
4 RCO = linoleyl, R^1 = H, linoleamide (9,12-octadecadienamide, ODDA)
5 RCO = oleoyl, R^1 = OH, oleyl hydroxamic acid (OHA)
6 RCO = linoleyl, R^1 = H, linoleyl hydroxamic acid (LHA)
hydrolysis of **3** and **4**
hydrolysis of **5** and **6**

Scheme 2. The possible metabolic pathway of endogenous fatty acid amides (FAAs) and FHAs to corresponding metabolites *via*: a) *N*-hydroxylation, b) *N*-dealkylation, and c) hydrolysis.

While *N*-hydroxyilation of aromatic amides by CYP enzymes to corresponding hydroxamic acids is common reaction [34], the *N*–hydroxylation of aliphatic amides is not usual therefore the potential formation of OHA and LHA from endogenous amides (**1** – **4**) will not be possible (Scheme 2, pathway **a**). On the other hand, OA and LA can be formed by CYP enzymes from OEA and LEA, respectively *via* *N*-dealkylation of amides **1** and **2** (Scheme 2, pathway **b**). All these endogenous and xenobiotic substances (**1** – **6**) bearing the -C(=O)NH)- moiety are subject to hydrolysis by FAAH (Scheme 2, pathway **c**).

Table 2. The biological targets for OHA, LHA, as well as for histone deacetylase inhibitor SAHA (suberoylanilide hydroxamic acid, vorinostat) predicted by SwissTargetPrediction.

		Probability (P)		
Target class	Target	OHA	LHA	SAHA
Membrane receptor	Cannabinoid receptor 1	0.6	0.8	
Membrane receptor	Cannabinoid receptor 2	0.4	0.3	
Enzyme	Fatty-acid amide hydrolase 1	0.6	0.5	
Enzyme	Histone deacetylase 1 to 11	0.4 -0.5 [1]	0.4 - 0.5 [1]	1.0

 doi:10.20944/preprints201711.0082.v1

Enzyme	Corticosteroid 11-beta-dehydrogenase isozyme 1 and 2	0.3	0.3	
Enzyme	Hydroxysteroid 11-beta-dehydrogenase 1-like protein		0.3	
Ion channel	Transient receptor potential cation channel subfamily V member 1	0.3		
Enzyme/Unclassified	Complex			1.0
Serine protease	Lipid-phosphate phosphatase			0.6
Enzyme	FAD-linked sulfhydryl oxidase ALR			0.6
Metallo protease	22 kDA interstitial collagenase			0.5

[1] Histone deacetylase 1 to 9 (HDAC1 to HDAC9)

[2] Fatty acid-binding protein liver/Unclassified

2.3.2. ADMET properties prediction and safety profile of OHA and LHA

Although many studies have been published on the preparation and biological evaluation of FHAs obtained from plant oils, there is insufficient evidence about their safety profile. Therefore, the results of an oral administration of FHA from *Cyperus esculentus* seed oil in rats receiving a dose of 5 mg/kg/day showed no adverse effects [32]. However, in rats receiving a dose of 15 mg/kg/day (the least observed adverse effect level) a significant increase in alkaline phosphatase activity and triglycerides and creatinine levels were observed together with moderate hyper-albuminemia and hypoalbuminemia that resulted in an increased albumin/globulin ratio. In addition, the study on the aquatic toxicity of the golden algae *Prymnesium parvum*, implicated in fish and aquatic animal deaths globally revealed six fatty acid amides (FAAs) and LHAs as the toxins responsible for the observed aquatoxicity [58]. The poor pharmacokinetics and toxicity are important causes of costly late-stage failures in drug development and these areas should be considered as early as possible in the drug discovery process. Therefore, early data on absorption, distribution, metabolism, excretion and toxicity (ADMET) are needed. Regarding the aforementioned issues, *in silico* approaches are valuable tools as they increase our ability to predict and model the most relevant pharmacokinetic, metabolic, and toxicity endpoints that accelerate the drug discovery process [59].

In this study, FHAs were screened for undesirable ADMET properties *in silico*, using the liability scoring system known as ADMET Risk™ (ADMET Predictor™ 8.1, Simulations Plus, Inc., USA). Here we report the results of this *in silico* study in which the ADMET properties relevant to the toxic profile of OHA and LHA, the main components of the FHA mixture, were predicted by ADMET Predictor™ [60]. The obtained results were compared with the predicted parameters obtained for their precursor fatty acids (OA and LA). Since HDACs were predicted as potential biological targets of OHA and LHA (with probabilities P = 0.4 – 0.5), SAHA (P = 1.0) was also included *in silico* study. The results are presented in Table 3. In addition to these predicted data, the ADMET Predictor Metabolism Module (Human Cytochrome P450) which contains two models (the classification of compounds as general inhibitors of 5 major CYP isoforms and the qualitative and quanitative inhibition models for CYP3A4 with either midazolam or testosterone as the substrate) predicted the extensive LHA CYP metabolism in comparison to other investigated molecules. Thus

 doi:10.20944/preprints201711.0082.v1

sites of the CYP 1A2 metabolism in LHA were predicted at the following C-atoms with corresponding hydroxylated metabolites: C18* (ω), C17* (ω-1), C16* (ω-2), C14*, and C11* and additionally, a site of CYP3A4 at C8*. The predicted CYP metabolism of OA and LA by CYP 2E1 and CYP 1A1, respectively, involved the hydroxylation of corresponding C-atoms in each molecule: C18 and C18* (ω), C17 and C17* (ω-1), as well as C16 and C16* (ω-2). Interestingly, for OHA no atoms were predicted to be sites of the CYP metabolism. The main sites (C-atoms) of the CYP metabolism of SAHA were aromatic C-atoms at positions *ortho* and *para* (C2′ and C4′, respectively) towards the alkyl chain substitution in the SAHA molecule. The ADMET analysis predicted the inhibition of the testosterone (ti) metabolism by CYP 3A4 for LHA and LA as well as SAHA.

Both pairs, *i.e.*, OHA and LHA as well as OA and LA were characterized by high lipophilicity (MlogP = 4.141 to 4.261) compared to the lipophilicity of SAHA (MlogP = 2.057) (Table 3). The low absorption scores expressed as S-Absn Risk (Table 3) were predicted for all of the investigated molecules and the highest score was obtained for OA (S-Absn Risk = 3). The common predicted parameters of overall ADMET risk for all of the investigated molecules (except for SAHA) according to these predictions corresponded to the big number of rotational bonds (RB), lipophylicity (ow, Mlog) and water solubility (Sw).

TOX Risk™, the toxicity liability score composed of 7 rules (hERG, acute rat toxicity, rat and mouse carcinogenicity, hepatoxicity, liver enzyme elevation, and Ames mutagenicity) predicted the highest score of 3 that corresponded to hepatotoxicity (SG and Hp) and mutagenicity (Mu) for LHA, the score of 2 for SAHA (Hp and Mu) and the lowest score of 1 for OHA, OA and LA (Mu, Hp and Hp, respectively) (Table 3).

On the basis of an *in silico* Amest test of the ADMET Predictor™ modules, mutagenicity in *S. typhimurium* was predicted for hydroxamic acids (OHA, LHA and SAHA) and not for carboxylic acids (OA and LA) which implies that CONHOH moiety contributes to the potential mutagenic effect of the FHAs.

Regarding the environmental toxicity observed with LHA [58], in this study biodegradable toxicity was predicted for all of the investigated molecules except for SAHA. The environmental toxicity as a consequence of a high bioconcentration factor (BCF) defined as the ratio of the chemical concentration in biota to that in water at steady state, as a result of absorption *via* the respiratory surface, was predicted to be as follows: TOX BCF™ of LA (48.945) > OA (31.734) > LHA (6.280) > OHA (4.453) > SAHA (1.275) (Table 3).

On the basis of the predicted TOX Risk™ scores, as well as overall ADMET Risk™ scores displayed in this order: LHA (6.846) > LA (5.987) > OA (5.000) > OHA (4.130) > SAHA (3.197), it can be concluded that LHA is the most toxic molecule in this study with the worse safety profile (Table 3).

Table 3. Computed molecular descriptors and the predicted ADMET properties of FHAs *i.e.*, OHA and LHA, for their corresponding precursor fatty acids, oleic and linoleic acid (OA and LA, respectively) and SAHA (suberoylanilide hydroxamic acid, vorinostat) by ADMET Predictor™ [60]

Acid	M_r [1]	MlogP [2]	ADMET Risk[3]	ADMET Code	CYP Risk[4]	CYP Code	TOX MUT Risk[5]	TOX MUT Code	TOX Risk[6]	TOX Code	S-Absn Risk[7]	S-Absn Risk Code	TOX Rat [17]	TOX BRM Rat [18]	TOX BRM Mouse [19]	BCF [20]
OHA	297.484	4.238	4.130	RB [8], ow [9], Sw [10], fu [11], Mu [12]	0	None	2	m1 [20], S2 [21]	1	Mu	2.966	RB, ow, Sw	4015.411	111.181	1034.993	4.453
LHA	295.468	4.141	6.846	RB, ow, Sw, SG [13], Hp [14] Mu, 1A [15], ti [16]	1.225	1A, ti	2	m1, S2	3	SG, Hp, Mu	2.621	RB, ow, Sw	2722.121	79.991	1056.419	6.28
OA	282.470	4.261	5.000	RB, ow, Sw, fu, Hp	0	None	0	None	1	Hp	3.000	RB, ow, Sw	7019.417	536.652	743.482	31.734
LA	280.454	4.165	5.987	RB, ow, Sw, fu, Hp, ti	1.000	ti	0	None	1	Hp	1.000	RB, ow, Sw	5050.166	411.214	761.805	48.945
SAHA	297.484	2.057	3.197	RB, Hp, Mu, 1A	0.697	1A	2	m1, S2	2	Hp, Mu	0.500	RB	1460.041	10.165	1522.536	1.275

[1] Relative molecular mass; [2] Lipophilicity (according to Moriguchi); [3] Overall ADMET toxicity; [4] Risk of the toxicity due to biotransformation by CYP enzymes; [5] The risk of mutagenicity in *S. Typhimurium*; [6] Risk of overall toxicity, including mutagenicity; [7] Low absorption risk; [8] RB – number of rotatable bonds (too flexible); [9] ow S+logP, S+logD at pH 7,4 and MlogP (too lipophilic); [10] Sw (low water solubility); [11] fu –low fraction unbound in plasma; [12] Mu – mutagenicity in a panel of *in silico* Ames tests with and without metabolic activation; [13] SG – hepatotoxicity based on another kind of serum enzyme profile; [14] Hp – hepatotoxicity based on one kind of serum enzyme profile; [15] excessive clearance by CYP 1A2; [16] ti – inhibition of testosterone metabolism by CYP 3A4. [17] Acute lethal toxicity in rat, the TD_{50} value of a particular compound in units of mg/kg/day; [18] TD_{50} value of a particular compound in units of mg/kg/day, TD_{50} – dose of a substance administered orally to rats over the course of their lifetimes that results in the appearance of tumours in 50% of their population); [19] TD_{50} value in mice mg/kg/day; [20] BCF – environmental bio-concentration factor;

doi:10.20944/preprints201711.0082.v1

 doi:10.20944/preprints201711.0082.v1

4. Materials and Methods

The olive oil from autochthonous Croatian olive cultivars was donated from a producer in the town of Brela (Dalmatia, Croatia) and it served as the main source material for the preparation of the FHAs. Reagents, starting materials and solvents were purchased from common commercial suppliers: sodium hydroxide p.a. from Kemika (Croatia), hydroxylamine hydrochloride p.a., ferric (III) chloride and hydrochloric acid 37% from Merck (Germany), methanol for HPLC, hexane p.p.a. and dichloromethane p.p.a. from Sigma-Aldrich (Germany). Butylated hydroxyanisole (BHA), 2,2-diphenyl-1-picrylhydrazyl (DPPH), β-carotene, linoleic acid, Tween-40 (polyoxyethylene sorbitan monopalmitate) and quercetin were purchased from Sigma-Aldrich Chemical Co. (USA). The other chemicals and solvents used in this study were of analytical grade. Precoated Merck silica gel 60 F_{254} plates were used for thin-layer chromatography. The HeLa (ATCC® CCL-2™) tumor cell line (human, cervix, epithelial adenocarcinoma) and BJ (ATCC® CRL-2522™) normal cell line (human, skin, foreskin, fibroblast) were purchased from American Type Culture Collection, Manassas, VA, USA.

The melting point was determined at Stuart SMP3 melting point (Bibby Sterilin Ltd, Stone, Strafkodshire, UK) and is uncorrected. Mid-IR (MIR) spectra were recorded in KBr pellets using ABB Bomem MB102 Fourier-transform infrared spectrometer (Quebec, Canada). The FT Raman spectrum was recorded on a Bruker Equinox 55 IR spectrometer (Germany) equipped with a FRA 106/S module and Nd-YAG laser (1064 nm the wavelength of excitation). 1D and 2D homo- and hetero-nuclear ^{1}H- and ^{13}C-NMR spectra were recorded on a Bruker-Avance 600 MHz NMR spectrometer (Germany) operating at 600.133 MHz for the ^{1}H nucleus and 150.917 MHz for the ^{13}C nucleus. Samples were measured from $CDCl_3$ solution at 25 °C (298 K). Chemical shifts (δ) are in ppm, and are referred to the tetramethylsilane (TMS). The following 1D and 2D measurement techniques were used: standard ^{1}H and ^{13}C gated proton decoupling, APT, COSY, HMQC and HMBC. The 2D NMR spectra were measured in pulsed field gradient mode (z-gradient). Theoretical NMR data were computed for OHA and LHA using nmrshiftdb (http://nmrshiftdb.nmr.uni-koeln.de) and ChemDraw Ultra v. 11.0 ^{13}C NMR software packages. The analyses of the FHAs were achieved using matrix-assisted laser desorption/ionization time-of-flight/time-of flight mass spectrometry (MALDI TOF/TOF MS). A model 4800 Plus MALDI TOF/TOF analyser (Applied Biosystems Inc., Foster City, CA, USA) equipped with the Nd:YAG laser (355 nm wavelength frequency 200 Hz and the pulse of 3-7 ns) was used. Colorimetric measurements were made by an Elisa microplate reader (iMark, BIO RAD, Hercules, CA, USA). Biological targets were predicted using the SwissTargetPrediction web server at http://www.swisstargetprediction.ch/ and ADMET properties were predicted using ADMET Predictor™ (Simulations Plus, USA).

4.1. Synthesis of fatty hydroxamic acids (FHAs)

To a solution of olive oil (1.00 g) in hexane (15 mL), 5 mL of 2 M hydroxylamine in methanol solution prepared according to a previously published procedure [39] was added (Scheme 1). The reaction mixture was stirred at 130 rpm and 72 °C for 5 h and then at room temperature for 15 h.

Preprints (www.preprints.org) | NOT PEER-REVIEWED | Posted: 14 November 2017 doi:10.20944/preprints201711.0082.v1

The residue was filtered off and the hexane layer was separated and washed with 2 M HCl and water, dried over sodium sulphate, and evaporated in a vacuum. The crude product was purified by column chromatography (silica gel, dichloromethane/methanol, 9:1) to obtain the FHA product as a white solid residue (100 mg/g, expressed in mg per 1 g of olive oil). Following isolation and purification, the qualitative analysis test was performed by addition of iron (III) ions dissolved in hydrochloric acid to the solution of FHAs in methanol and the resulting purple coloured complex indicated the presence of hydroxamic acid groups.

4.2. Characterization of fatty hydroxamic acids by spectroscopic methods

Fatty hydroxamic acid mixture: white solid; m.p. 64-69 °C;
FT-IR (KBr) ν_{max}: 3285 (-NH-OH), 3001 (-CH=CH-), 2952 ($-CH_3$), 2918 ($-CH_2-$), 1664 (-CO-, amide I), 1624 (-CO-, amide II) cm^{-1}; data see in Table S-1 in the supplementary material;
Raman (ν_{max}/ cm^{-1}): data see in Table S-1 in the supplementary material.
^{1}H-NMR ($CDCl_3$, 600 MHz) data see in Table S-2 and Figure S-2 in the supplementary material
^{13}C-NMR ($CDCl_3$, 150 MHz) data see in Table S-2 and Figure S-3 in the supplementary material
MALDI TOF/TOF MS: m/z 320 (100) $[M_{OHA} + Na]^+$, m/z 318 (25) $[M_{LHA} + Na]^+$; all data see in Fgure 2 and Figure S-7 in the supplementary material).

4.3. Biological evaluation in vitro

4.3.1. Antioxidant activity

Free radical scavenging activity (*RSA*) was evaluated by the scavenging of 1,1-diphenyl-2-picrylhydrazyl (DPPH) radicals according to a previously described method [61] with some modifications. A methanolic solution of DPPH (20 µL, 0.735 mg/mL) was added to 130 µL of either methanol (negative control) or FHA methanolic solutions of various concentrations. The mixture was vortexed for 1 min and then left to stand at room temperature in the dark. After 30 min absorbance was read at 545 nm. A standard antioxidant, the butylated hydroxyanisole (BHA), was used as positive control. RSA was expressed as the concentration that scavenges 50% of DPPH free radicals (EC_{50}). RSA was calculated using the following equation:

$$X(\%) = \frac{A_{control} - A_{sample}}{A_{control}} \cdot 100$$ (Equation 1), where *X* represents the RSA in percentage (%)

while $A_{control}$ is methanol and A_{sample} is FHAs solution in methanol. The concentration of FHAs sample that provides 50 % inhibition (EC_{50}) was calculated by plotting the inhibition percentages against the concentrations of the sample.

The chelating activity (*ChA*) of FHAs toward ferrous ions (Fe^{2+}) was studied according to modified literature procedures [62]. In brief, to an aliquot of the methanolic solution of FHAs (150 µL), 0.25 mM $FeCl_2$ solution (50 µL) was added. After 5 min, the reaction was initiated by adding 1.0 mM ferrozine solution (100 µL). Absorbance at 545 nm was recorded after 10 min of incubation at room temperature. A reaction mixture containing methanol (150 µL) instead of FHA solution

 doi:10.20944/preprints201711.0082.v1

served as control. Quercetin (Qn) and EDTA were used as the chelating standards. The chelating activity (*ChA)* was expressed as the concentration that chelates 50% of Fe^{2+} ions (EC_{50}). ChA was calculated using Equation 1, where *X* represents ChA while $A_{control}$ is the absorbance of the negative control, *i.e.,* blank solution without test compound and A_{sample} is the absorbance of the FHAs solution in methanol.

The antioxidant activity (AOA) in β-carotene-linoleic acid assay of FHAs was evaluated as described previously [62]. Tween 40 (200 mg) and β-carotene solution in chloroform (1.0 mL, γ = 0.2 mgL^{-1}) were mixed. After removing chloroform in a rotary evaporator, linoleic acid (20 mg) and aerated distilled water (30 mL) were added to the oily residue with vigorous stirring. Aliquots (200 µL) of the thus obtained emulsion were added to sample solutions in methanol (50 µL). After adding the emulsion to the FHA solution in methanol (sample solution), the reaction mixture was incubated at 50 °C for 1 h. During that period, the absorbance was measured at 450 nm at 15-minute intervals, starting immediately after sample preparation (*t* = 0 min) until the end of the experiment (*t* = 120 min). A reaction mixture containing methanol (50 µL) instead of the sample solution served as control. Butylated hydroxyanisol (BHA) was used as an antioxidant standard. The antioxidant activity was calculated using Equation 1 where *X* represents AOA, while $R_{control}$ and R_{sample} are the average bleaching rates of the water control and antioxidant (test compound or BHA standard), respectively.

The reducing power (RP) assay of FHAs was conducted as previously described [63] with some modifications. In brief, each FHA solution of different concentrations (0.1 – 0.5 mg/mL) in distilled water (0.5 mL) was mixed with 1.25 mL of 0.2 M sodium phosphate buffer (pH 6.6) and 1.25 mL of 1% (mv) potassium ferricyanide. The mixture was incubated for 20 min at 50°C after which 1.25 mL of 10% trichloroacetic acid (m/v) was added and the mixture was centrifuged at 2795 rpm. The upper layer (1.25 mL) was mixed with 1.25 mL of deionized water and 0.25 mL of 0.1% (m/v) ferric chloride. Absorbance was measured at 700 nm against water as a blank. Ascorbic acid was used for comparison.

Statistical analysis. All assays regarding *antioxidant activity* were performed in triplicate. The results are expressed as mean ± SD. Statistical comparisons were made using Student's t-test or one-way ANOVA, followed by Dunnett's *post-hoc* test for multiple comparison with the control. Statistical analyses were performed using the JMP V6 from SAS software (SAS Institute, Cary, NC, USA).

4.3.2. Cytotoxic *activity*

Cytotoxic effects were determined by MTT [(3-(4,5-dimethylthiazol-2-yl)-2,5-diphenyl tetra sodium bromide)] assay *in vitro* [64]. MTT is a pale yellow substrate that cleaved by living cells to yield a dark blue formazan product in a process that requires active mitochondria. Thus the amount of cleaved MMT is directly proportional to the number of viable cells present, which is quantified by colorimetric methods. The experiments were carried out on one normal human cell line (ATCC® CRL-2522™) of foreskin fibroblast (BJ) between 28-29 passages and one epithelial tumour cell line (cervix adenocarcinoma - HeLa, ATCC® CCL-2™HeLa). Cells were cultured in Dulbecco's modified Eagle medium – DMEM (Gibco) supplemented with 10% heat-inactivated foetal bovine serum (FBS, Gibco, EU), 2 mM glutamine, and 100 U/0.1mg penicillin/streptomycin. All cells were grown as

Preprints (www.preprints.org) | NOT PEER-REVIEWED | Posted: 14 November 2017 doi:10.20944/preprints201711.0082.v1

monolayer in tissue culture flasks (BD Falcon, Germany) in humidified atmosphere under the conditions of 37 °C/5% of CO_2 gas in a CO_2 incubator (Shell Lab, Sheldon Manufacturing, USA). The trypan blue dye exclusion method was used to assess the cell viability.

The FHA sample was prepared as a stock solution (5 mg/mL) in DMSO. Working solutions (0.005 up to 5 mg/mL) were made in purified water prior to the experiment. Cells were seeded in 96 micro well flat bottom plates (Greiner, Frickenhausen, Austria) at concentration $2x10^4$ cells/mL and left overnight in the CO_2 incubator allowing them to attach to the plate surface. After 72 h the compound addition growth medium was discarded and 5 mg/mL of MTT was added. After 4 h incubation at 37 °C the water insoluble MTT-formazan crystals were dissolved in DMSO. Absorbance was measured at 595 nm on an Elisa microplate reader (iMark, BIO RAD, Hercules, CA, USA). Controlled, the cells were grown under the same conditions and treated with appropriate concentration of solvent used for the preparation of the tested compound. All experiments were performed at least three times in triplicate. The percentage of cell growth (*PG*) was calculated using the following equation

$$PG = \frac{A - A_{blank}}{A_{control} - A_{blank}} \cdot 100$$ (Equation 2), where A means absorbance of FHAs solution, the blank medium is medium without cells containing MTT and DMSO while control is cell containing DMSO.

The GI_{50} value, defined as compound concentration (mg/mL) leading to cellular viability reduction by 50%, was calculated and used as a parameter to compare cytotoxicity among the tested substances. STATISTICA 11 software and Kolmogorov-Smirnov two-sample tests were used to statistically evaluate the data obtained from the MTT test.

4.3.3. In silico *prediction of biological targets and ADMET properties*

4.3.3.1. In silico *prediction of biological targets*

Biological on- and off-targets of OH, LHA, OA, LA and SAHA were predicted using SwissTargetPrediction, a web server accessible free of charge and without login requirement at http://www.swisstargetprediction.ch/.

4.3.3.1. In silico *prediction of ADMET properties*

ADMET properties of OHA, LHA, OA, LA and SAHA were evaluated using ADMET Predictor™ Version 8.1 (Simulations Plus Inc., USA).

5. Conclusions

FHAs were synthesized by hydroxylaminolysis from olive oil triacylglycerides as starting material. The obtained spectroscopic data revealed that the isolated product corresponds to the FHAs mixture of OHA and LHA (ratio 4:1). The results of preliminary *in vitro* assays and antitumor activity (HeLa cell line) revealed that the FHA mixture possessed moderate antioxidant and antiradical properties, as well as antitumor activity. The results of biological activity testing and computed data for FHAs highlighted OHA and LHA as promising lead-compounds for further research.

Although many hydroxamic acid-based HDAC inhibitors are currently in discovery and preclinical phases, the number of HDACIs that have been approved for the market, still remains low. Hence, there is permanent interest in the synthesis of new hydroxamic acid derivatives and their biological evaluation, so any new chemical entity in this class can be considered for investigation as a potentially new active drug.

Supplementary Materials: Figure S1: A parallel display of FTIR spectra of olive oil recorded as liquid on potassium bromide (KBr) pellet (**A**) and fatty hydroxamic acids (FHAs) recorded in potassium bromide (KBr) pellet (**B**), **Figure S2**: The ^{1}H-NMR spectrum of FHAs mixture recorded in $CDCl_3$ and chemical structures of its main components, *i.e.*, OHA and LHA with indicated signals for each proton groups, **Figure S3**: ^{13}C-NMR spectrum of fatty hydroxamic acid (FHAs) mixture and chemical structures of its main components, *i.e.*, oleoyl and linoleyl hydroxamic acid (OHA and LHA, respectively) with labeled C-atoms, **Figure S4**: The 2D NMR HMQC (Heteronuclear Multiple Quantum Coherence) spectrum of FHAs in the region of aliphatic and olefinic protons displaying correlations through one bond. (The signal at 77.0 ppm (13C-NMR) and 7.24 ppm (^{1}H-NMR) belong to $CDCl_3$ solvent), **Figure S5**: A part of 2D NMR HMBC (Heteronuclear Multiple Bond Coherence) spectrum of FHAs displaying correlations through multiple bonds in the region of aliphatic and olefinic protons, **Figure S6**: A part of ^{1}H-^{1}H-COSY spectrum of FHAs in the region of aliphatic and olefinic protons, **Figure S7**: A MALDI-TOF/TOF tandem mass spectrum of FHAs mixture representing the region of unsaturated fatty hydroxamic acids, *i.e.*, m/z 310 – 323 with molecular ions of OHA and LHA as their sodium alkali adducts $[M + Na]^+$, $[M + Na + H]^+$ and $[M + Na + 2H]^+$, **Table S1.** The list of vibrational frequencies and their assignments in FTIR (KBr) and Raman spectra of recorded FHAs, **Table S2.** ^{13}C- and ^{1}H-NMR spectroscopic data (recorded at 175 and 700 MHz, respectively; $CDCl_3$) of fatty hydoxamic acids mixture (FHAs) consisted of oleoyl (OHA) and linoleyl hydroxamic acid (LHA*) and theoretical[2,3] spectral data of OHA and LHA* and literature spectral data of LHA.

Acknowledgments: The authors thank Zdravko Pervan (Brela, Croatia) for the donation of olive oil and Snežana Miljanić (University of Zagreb, Faculty of Science, Chemistry Division) for enabling us the use of the Raman spectrometer. The authors also thank Professor Stanko Uršić for his support and valuable suggestions during the work as well as all the members of the Department of Physical Chemistry, University of Zagreb, Faculty of Pharmacy and Biochemistry. This study was supported by the Ministry of Science, Education and Sports of the Republic Croatia (Grants: 006-0063082-0354, 006-0982929-2940, 098-0982929-2917 and 219-0982914-217).

Author Contributions: M.B. conceived, designed and performed the synthetic part of experiments, reviewed the literature data and prepared the subfinal and helped in preparing manuscript for publication; D.V.T. conceived and designed NMR experiments and analysed NMR and MS spectra and contributed to structure elucidation; Ž.M. performed the NMR experiments and contributed reagents, materials and analysis tools; M.Z.K. designed and performed antioxidative and chelating activity and wrote the corresponding part of the manuscript; D.B. performed and analysed the FTIR and Raman spectra; K.M.Š. and M.B.L. performed and wrote the cytotoxic activity segment; M.J.M.T. analysed the overall data and contributed to spectral structures elucidation, designed and performed *in silico* studies, wrote the manuscript and prepare the paper for publication; All of the authors read and approved the final manuscript.

Conflicts of Interest: The authors declare no conflict of interest.

References

1. McAllister, L.A.; Montgomery, J.I.; Abramite, J.A.; Reilly, U.; Brown, M.F.; Chen J.M.; Barham, R.A.; Che, Y.; Chung, S.W.; Menard, C.A.; Mitton-Fry, M.; Mullins, L.M.; Noe, M.C.; O'Donnell, J.P.; Oliver, III R.M.; Penzien, J.B.; Plummer, M.; Price, L.M., Shanmugasundaram, V.; Tomaras, A.P.; Uccello, D.P. Heterocyclic methyl sulfone hydroxamic acid LpxC inhibitors as Gram-negative antibacterial agents. *Bioorg Med Chem Lett* **2012**, 22, 6832–6838, DOI: 10.1016/j.bmcl.2012.09.058.
2. Guo, B.; Zhang, Y.; Li, S.; Lai, T.; Yang, L.; Chen, J.; Ding, W. Extract from Maize (*Zea mays* L.): Antibacterial activity of DIMBOA and its derivatives against *Ralstonia solanacearum*. *Molecules* **2016**, 21, 1397-1409, DOI: 10.3390/molecules21101397.
3. Rao, M.J.; Sethuram, B.; Rao, T.N. Synthesis and spectroscopic and fungicidal characterization of hydroxamic acids and their metal chelates *J Inorg Biochem* **1985**, 24, 155-160, DOI: 10.1016/0162-0134(85)80007-6.
4. Bravo, H.R.; Lazo, W. Antialgal and antifungal activity of natural hydroxamic acids and related compounds. *J Agric Food Chem* **1996**, 44, 1569–1571. DOI: 10.1021/jf950345e.
5. Haron, M.J.; Jahangirian, H.; Ismail, M.H.S.; Rafiee-Moghaddam, R.; Rezay, M.; Shameli, K.; Gharayebi, Y.; Abdollahi, Y.; Peyda, M.; Mahdavi, B. Antifungal properties of phenyl fatty hydroxamic acids and their copper complexes synthesized based on canola and palm kernel oils. *Asian J Chem* **2013**, 25, 4183-4188, DOI: 10.3390/ijms13022148.
6. Yoshida, M.; Furumai, R.; Nishiyama, M.; Komatsu, Y.; Nishino, N.; Horinouchi, S. Histone deacetylase as a new target for cancer chemotherapy. *Cancer Chemoth Pharm* **2001**, 48, 20-26, DOI: 10.1007/s002800100300.
7. Barbarić, M.; Uršić, S.; Pilepić, V.; Zorc, B.; Hergold-Brundić, A.; Nagl, A.; Grdiša, M.; Pavelić, K.; Snoeck, R.; Andrei, G.; Balzarini, J.; De Clercq, E.; Mintas, M. Synthesis, X-ray crystal structure study, and cytostatic and antiviral evaluation of the novel cycloalkyl-*N*-aryl-hydroxamic acids. *J Med Chem* **2005**, 48, 884-887, DOI: 10.3390/molecules16086232.
8. Guan, P.; Sun, F.; Hou, X.; Wanga, F.; Yi, F.; Xu, W.; Fang, H. Design, synthesis and preliminary bioactivity studies of 1,3,4-thiadiazole hydroxamic acid derivatives as novel histone deacetylase inhibitors. *Bioorg Medl Chem* **2012**, 20, 3865–3872, DOI: 10.1016/j.bmc.2012.04.032.
9. Zhu, Y.; Chen, X.; Wu, Z.; Zheng, Y.; Chen, Y.; Tang, W.; Lu, T. Synthesis ad atitumor activity of novel diaryl ether hydroxamic acid derivtives as potential HDAC inhibitors. *Arch Pharm Res* **2012**, 35, 1723-1732, DOI: 10.1007/s12272-012-1003-0.
10. Pal, D.; Saha, S. Hydroxamic acid - A novel molecule for anticancer therapy, *J Adv PharmTechnol Res* **2012**, 3, 92–99, DOI:10.4103/2231-4040.97281.
11. Yuan, Z.; Sun, Q.; Li, D.; Miao, S., Chen, S.; Song, L; Gao, C.; Chen, Y.; Tan, C; Yiang, Y. Design, synthesis and anticancer potential of NSC-319745 hydroxamic acid derivatives as DNMT and HDAC inhibitors. *Eur J Med Chem* **2017**, 134, 281-292, DOI: 10.1016/j.ejmech.2017.04.017.
12. Muri, E.M.F.; Nieto, M.J.; Sindela, R.D.; Williamson, J.S. Hydroxamic acids as pharmacological agents. *Curr Med Chem* **2002**, 9, 1631–1653, DOI: 10.2174/0929867023369402#sthash.AEQqE6Yu.dpuf.
13. Kleemann, A.; Engel, J.; Kutscher, B.; Reichert, D. Pharmaceutical Substances: Syntheses, Patents, Applications, 4th Ed. Georg Thieme Verlag, Stuttgart, **2001**, 2521, ISBN: 3-13-558404-6.
14. Ugwu, D.I.; Ezema, B.E.; Eze, F.U.; Ayogu; J.I.; Ezema, C.G.; Ugwuj, D.I. Synthesis and biological applications of hydroxamates. *Am J Org Chem* **2014**, 4, 26-61, DOI: 10.5923/j.ajoc.20140402.02.
15. Dokmanovic, M.; Clarke, C.; Marks, P.A. Histone deacetylase inhibitors: overview and perspectives, *Mol Cancer Res* **2007**, 5, 981-989. DOI: 10.1158/1541-7786.MCR-07-0324.
16. Thurn, K.T.; Thomas, S.; Moore, A.; Munster, P.M. Rational therapeutic combinations with histone deacetylase inhibitors for the treatment of cancer. *Future Oncol* **2011**, 7, 263-283, DOI: 0.2217/fon.11.2.
17. Manal, M.; Chandrasekar, M.J.; Gomathi, P.J.; Nanjan, M.J. Inhibitors of histone deacetylase as antitumor agents: A critical review. *Bioorg Chem* **2016**, 67, 18–42, DOI: http://dx.doi.org/10.1016/j.bioorg.2016.05.005.
18. Nebbioso, A.; Carafa, V.; Benedetti, R.; Altucci, L. Trials with 'epigenetic'drugs: an update. *Mol Oncol* **2012**; 6, 657-682, DOI: 10.1016/j.molonc.2012.09.004.

19. Fournand, D.; Vaysse, L.; Dubreucq, E.; Arnaud, A.; Galzy, P. Monohydroxamic acid biosynthesis. *J Mol Catal B-Enzym* **1998**, 5, 207–211, DOI: 10.1016/S1381-1177(98)00036-8.
20. Hoidy, W.H.; Ahmad, M.B.; Al-Mulla, E.A.J.; Yunus, W.M.Z.; Ibrahim, N.A. Synthesis and characterization of fatty hydroxamic acids from triacylglycerides, *J Oleo Sci* **2010**, 59, 15-19, DOI: http://doi.org/10.5650/jos.59.15.27.
21. Porcheddu, A.; Giacomelli, G. Synthesis of oximes and hydroxamic acids. In The chemistry of hydroxylamines, oximes and hydroxamic acids, Rapport, Z; Liebman, J. F. Eds., John Wiley and Sons, **2009**, p.p. 163-231, ISBN 978-0-470-51261-6.
22. Brodowsky, I.D.; Hamberg, M.; Oliw, E.H. BW A4C and other hydroxamic acids are potent inhibitors of linoleic acid 8R-dioxygenase of the fungus *Gaeumannomyces graminis*. *Eur J Pharmacol* **1994**, 254, 43–47, DOI: 10.1016/0014-2999(94)90368-9.
23. Butovich, I.A.; Reddy, C.C. Inhibition of potato lipoxygenase by linoleyl hydroxamic acid: kinetic and EPR spectral evidence for a two-step reaction. *Biochem J* **2002**, 365, 865–871, DOI: 10.1042/BJ20020495.
24. Butovich, I.A.; Lukyanova, S.M. Inhibition of lipoxygenases and cyclooxygenases by linoleyl hydroxamic acid: comparative in vitro studies, *J Lipid Res* **2008**, 49, 1284–1294, DOI: 10.1194/jlr.M700602-JLR200.
25. Raffiee-Moghaddam, R.; Salimon, J.; Haron, M.D.J.; Jahangirian, H. Jatropha Curcas seed oil as a new substrate for enzymatic methylhydroxylaminolysis. *Dig J Nanomater Bios* **2013**, 8, 415-422.
26. Jahangirian, H.; Haron, M.J.; Silong, S.; Yusof, N.A. Enzymatic synthesis of phenyl fatty hydroxamic acids from canola and palm oils. *J Oleo Sci* **2011**, 60, 281-286, DOI: http://doi.org/10.5650/jos.60.281.
27. Jahangirian, H.; Haron, M.J.; Yusof, N.A.; Silong, S.; Kassim, A.; Rafiee-Moghaddam, R.; Peyda, M.; Gharayebi, Y. Enzymatic synthesis of fatty hydroxamic acid derivatives based on palm kernel oil. *Molecules* **2011**, 16, 6634-6644, DOI: 10.3390/molecules16086634.
28. Suhendra, D.; Wan Yunus, W.M.Z.; Haron, M.J.; Basri, M.; Silong, S. Enzymatic synthesis of fatty hydroxamic acids from palm oil. *J Oleo Sci* **2005**, 54, 33-38, DOI: http://doi.org/10.5650/jos.54.33.
29. Jahangirian H.; Haron, J.; Silong, S.; Yusof, N.A.; Shameli, K.; Eissazadeh, S.; Rafiee Moghaddam, R. Mahdavi, B.; Jafarzade, M. Antibacterial effect of phenyl fatty hydroxamic acids synthesized from canola oil, *J Med Chem Plants Res* **2011**, 5, 4826-4831.
30. Jahangirian, H.; Haron, M.J.; Ismail, M.H.S, Raffie-Moghaddam, R.; Afsah-Hejri, L.; Abdollahi, Y.; Rezayi, M.; Vafaei, N. Well diffusion method for evaluation of antibacterial activity of cooper phenyl fatty hydroxamate synthesized from canola and palm kernel oils. *Dig J Nanomater Bios* **2013**, 8, 1263 – 1270.
31. Rafiee-Moghaddam, R.; Salimon, J.; Haron, M.J.; Jahangirian, H.; Ismail, M.H.S.; Afsah-Hejri, L.; Vafaei, N.; Tayefehchamani, Y. Application of Methyl Fatty Hydroxamic Acids Based on Jatropha Curcas Seeds oil and Their Metal Complexes as Antimicrobial Agents. *Dig J Nanomater Bios* **2014**, 9, 261-271.
32. Adewuyi, A.; Otuechere, C.A.; Oteglolade, Z.O.; Bankole, O.; Unuabonah, E.I. Evaluation of the safety profile and antioxidant activity of fatty hydroxamic acid from underutilized seed oil of *Cyperus esculentus*. *J Acute Dis* **2015**, 4, 230-235, DOI: http://dx.doi.org/10.1016/j.joad.2015.04.010.
33. Kovacic, P.; Edwards, C.L. Hydroxamic acids (therapeutics and mechanism): chemistry, acyl nitroso, nitroxyl, reactive oxygen species, and cell signaling, *J Recept Sig Transd* **2011**, 31, 10-19, DOI: 10.3109/10799893.2010.497152.
34. Koymans, L; Donne-Op den Kelder, G. M.; te Koppele, J. M.; Vermeulen, N P. E. Generalized cytochrome P-450-mediated oxidation and oxygenation reactions in aromatic substrates with activated N-H, O-H, C-H or S-H substituents, *Xenobiotics* **1993**, 23, 633-648.
35. Dipple, A.; Micheyda, C. J.; Weisburger, E. K. Metabolism of chemical carcinogens *Pharmacol Ther* **1985**, 27, 265-296.
36. Jadrijević-Mladar Takač, M.; Kos, I.; Biruš, M.; Butula, I.; Gabričević, M. A study of the physico-chemical properties of 1,3,5-trihydroxy-1,3,5-triazin-2,4,6[1H,3H,5H]-trione. *J Mol Struct* **2006**, 782, 24-31, DOI: 10.1016/j.molstruc.2004.09.018.
37. Kos, I.; Jadrijević-Mladar Takač, M.; Butula, I.; Biruš, M.; Maravić-Vlahoviček, G.; Dabelić, S. Synthesis, antibacterial and cytotoxic activity evaluation of hydroxyurea derivatives. *Acta Pharm* **2013**, 63, 175-191, DOI: 10.2478/acph-2013-0014.

38. Jakobušić-Brala, C.; Benčić, Đ.; Šindrak, Z.; Barbarić, M.;Uršić, S. Labeled extra virgin olive oil as food supplement, phenolic compound in oils from some autochtonic Croatian olives, *Grasas Aceites* **2015**, 66, e099, DOI: http://dx.doi.org/10.3989/gya.0228151.
39. Antonis, A. The colorimetric determination of ester groups in lipid extracts. *J Lipid Res* **1960**, 1, 485-486.
40. Boskou, D.; Blekas, G.; Tsimidou, M. Olive oil composition. In. *Olive Oil: Chemistry and Technology*, 2nd ed., Boskou, D., Ed., AOCS Press, Champaign, Ilinos, 2006; pp. 41 – 72; ISBN: 978-1-893997-88-2.
41. Arudi, R.L.; Sutherland, M.W.; Bielski, B.H.J. Purification of oleic acid and linoleic acid. *J Lipid Res* **1983**, 24, 485-488.
42. Vaysse, L.; Dubreucq, E.; Pirat, J.L.; Galzy, P. Fatty hydroxamic acid biosynthesis in aqueous medium in the presence of the lipase-acyltransferase from *Candida parapsilosis*. *J Bioteh* **1997**, 53, 41-46, DOI: 10.1016/S0168-1656(96)01660-4.
43. Shiao, T.Y.; Shiao, M.S. Determination of fatty acid composition of triacylglycerides by high resolution NMR spectroscopy. *Bot Bull Academia Sinica* **1989**, 30, 191-199.
44. Salinero, C.; Feás, X.J.; Mansilla, P.; Seijas, J.A.; Vázquez-Tato, M.P.; Vela, P.; Sainz, M.J. ^{1}H-Nuclear magnetic resonance analysis of the triacylglyceride composition of cold-pressed oil from *Camellia japonica*. *Molecules* **2012**, 17, 6716-6727, DOI: 10.3390/molecules17066716.
45. Reische, D.W.; Lillard, D.A.; Eitenmiller, R.R. Antioxidants. In *Food Lipids Chemistry Nutrition, and Biotechnology*, 3rd ed; Akoh, C.C., Min, D.B., Eds.; CRC Press: New York, NY, USA, 2008, pp. 409–433, ISBN-13: 978-1-4200-4663-2.
46. Galey, J.B. Recent advances in the design of iron chelators against oxidative damage. *Mini-Rev Med Chem* **2001**, 1, 233-242, DOI: 10.2174/1389557013406846.
47. Amarowicz, R.; Pegg, R.B.; Rahimi-Moghaddam, P.; Barl, B.; Weil, J.A. Free-radical scavenging capacity and antioxidant activity of selected plant species from the Canadian prairies. *Food Chem* **2004**, 84, 551–562; DOI: 10.1016/S0308-8146(03)00278-4.
48. Tyug, T.S.; Prasad, N.; Ismail, A. Antioxidant capacity, phenolics and isoflavones in soybean by-products. *Food Chem* **2010**, 123, 583–589, DOI: 10.1016/j.foodchem.2010.04.074.
49. Sarikurkcu, C.; Arisoy, K.; Tepe, B.; Cakir, A.; Abali, G.; Mete, E. Studies on the antioxidant activity of essential oil and different solvent extracts of *Vitex agnus castus* L. fruits from Turkey. *Food Chem Tox* **2009**, 47, 2479–2483, DOI: 10.1016/j.fct.2009.07.005.
50. Singh, N.; Rajini, P.S. Free radical scavenging activity of an aqueous extract of potato peel. *Food Chemistry* **2004**, 85, 611–616, DOI: 10.1016/j.foodchem.2003.07.003
51. Gfeller, D.; Michielin, O.; Zoete, V. Shaping the interaction landscape of bioactive molecules, *Bioinformatics* **2013**, 29, 3073-3079, DOI: 10.1093/bioinformatics/btt540.
52. Gfeller, D.; Grosdidier, A.; Wirth. M.; Daina, A.; Michelin, O.; Zoete, V. SwissTargetPrediction: a web server for target prediction of bioactive small molecules. *Nucl Acids Res* **2014**, 42, W32–W38, DOI: *10.1093/nar/gku293*.
53. De Petrocellis, L.; Cascio, M.G.; Di Marzo, V. The endocannabinoid system: a general view and latest additions. *B J Pharmacol* **2004**, 141, 765–774, DOI: 10.1038/sj.bjp.0705666.
54. McKinney, M.K.; Cravatt, B.F. Structure and Function of Fatty Acid Amide Hydrolase. *Annu Rev Biochem* **2005**, 74, 411–432, DOI:10.1146/annurev.biochem.74.082803.133450.
55. Leggett, J.D.; Aspley, S.; Beckett, S.R.G.; D'Antona, A.M.; Kendall, D.A.; Kendall, D.A. Oleamide is a selective endogenous agonist of rat and human CB_1 cannabinoid receptors. *Br J Pharmacol* **2004**; 141, 253–262, DOI: 10.1038/sj.bjp.0705607.
56. Thabuis, C.; Tissot-Favre, D.; Bezelgues, J. B.; Martin, J.C.; Cruz-Hernandez, C.; Dionisi, F.; Destaillats, F. Biological functions and metabolism of oleoylethanolamide. *Lipids* **2008**, 43, 887-894, DOI: 10.1007/s11745-008-3217-y.
57. Otrubova, K.; Ezzili, C.; Boger, D.L. The Discovery and Development of Inhibitors of Fatty Acid Amide Hydrolase (FAAH). *Bioorg Med Chem Lett. 2011*, 21, 4674–4685, DOI: 10.1016/j.bmcl.2011.06.096.
58. Bertin, J.M.; Zimba, P.V.; Beauchesne, R.K.; Huncik, M.K.; Moeller, D.R.P. Identification of toxic fatty acid amides isolated from the harmful alga *Prymnesium parvum* carter. *Harmful algae* **2012**, 20, 111-116, DOI: https://doi.org/10.1016/j.hal.2012.08.005.

59. Wang, Y.; Xing, J.; Xu, Y.; Zhou, N.; Peng, J.; Xiong, Z.; Liu, X; Luo, X.; Luo, C.; Chen, K., Zheng, M.; Jiang, H. In silico ADME/T modelling for rational drug design. Q Rev Biophys **2015**, 48, 488-515. DOI: 10.1017/S0033583515000190.
60. Lowless, M.S.; Waldman, M.; Franczkiewicz, R.; Clark, R.D. Using chemoinformatics in drug discovery. In *New approaches to drug discovery, Handbook of experimental pharmacology*, Nielsch, U., Fuhrmann, U., Jaroch, S., Eds.; Springer International Publishing AG: Switzerland **2016**; 232; 139-170, IS-13: 978-3319289120.
61. Yen, G.C.; Chen, H.Y. Antioxydant activity of various tea extracts in relation to their antimutagenicity. *J Agric Food Chem* **1995**, 43, 27-37. DOI: 10.1021/jf00049a007.
62. Rajić, Z.; Zovko Končić, M.; Milološa, K.; Perković, I.; Butula, I.; Bucar, F.; Zorc, B. Primaquine-NSAID twin drugs: Synthesis, radical scavenging, antioxidant and Fe^{2+} chelating activity. *Acta Pharmaceut* **2010**, 60, 325–337, DOI: 10.2478/v10007-010-0024-9.
63. Yen, G.C.; Chuang, D.Y. Antioxidant properties of water extracts from *Cassia tora* L. in relation to the degree of roasting. *J Agric Food Chem* **2000**, 48, 2760-276, DOI: 10.1021/jf991010q.
64. Mosmann, T. Rapid colorimetric assay for cellular growth and survival: application to proliferation and cytotoxicity assays. *J Immunol Methods* **1983**, 65, 55–63, DOI: *10.1016/0022-1759(83)90303-4*.